Laser Micromachining of Nanocomposite-Based Flexible Embedded Capacitors

Rabindra N. Das, Frank D. Egitto, John M. Lauffer and Voya R. Markovich
Endicott Interconnect Technologies, Inc., 1701 North Street, Endicott, New York, 13760.
Telephone No: 607-755-1389
E-mail: rabindra.das@eitny.com

Abstract

This paper discusses laser micromachining of barium titanate ($BaTiO_3$)-polymer nanocomposites and sol-gel thin films. In particular, recent developments on high capacitance, large area, and thin flexible embedded capacitors are highlighted. A variety of flexible nanocomposite thin films ranging from 2 microns to 25 microns thick were processed on copper or organic substrates by large area (13 inch X 18.5 inch, or 19.5 inch X 24 inch) liquid coating processes. SEM micrographs showed uniform particle distribution in the coatings. Nanocomposites resulted in high capacitance density (10-100 nF/inch^2) and low loss (0.02-0.04) at 1 MHz. The remarkably increased flexibility of the nanocomposite is due to uniform mixing of nanoparticles in the polymer matrix, resulting in an improved polymer-ceramic interface. $BaTiO_3$-epoxy polymer nanocomposites modified with nanomaterials were also fabricated and were investigated with SEM analysis. Capacitance density of nanomaterial-modified films was increased up to 500 nF/inch^2, about 5-10 times higher than $BaTiO_3$-epoxy nanocomposites. A frequency-tripled Nd:YAG laser operating at a wavelength of 355 nm was used for the micromachining study. The micromachining was used to generate arrays of variable-thickness capacitors from the nanocomposites. The resultant thickness of the capacitors depends on the number laser pulses applied. Laser micromachining was also used to make discrete capacitors from a capacitance layer. In the case of sol-gel thin films, micromachining results in various surface morphologies. It can make a sharp step, cavity-based wavy structure, or can make individual capacitors by complete ablation. Altogether, this is a new direction for development of multifunctional embedded capacitors.

Introduction

There has been increasing interest in the development of electronic circuits on flexible substrates to meet the growing demand for low-cost, large-area, flexible and lightweight devices, such as roll-up displays, e-papers, connectors, and keyboards. Organic materials have attracted a lot of attention for building large-area, mechanically-flexible electronic devices. These materials are widely pursued since they offer numerous advantages in terms of ease of processing, good compatibility with a variety of substrates, and great opportunity for structural modifications. Recently, much attention has been paid to Q-switched Nd:YAG laser-micromachining for MEMS/microsystems applications due to a number of advantages **[1]**. It is a single-step process with high flexibility, it does not contaminate the material being processed, and it allows highly localized treatment of materials with a spatial resolution of tens of microns. The present study describes a novel process that uses a computer controlled Nd:YAG laser system to create complex 3D micromachined embedded capacitors.

Nanocomposite-based embedded capacitors deserve special attention as they provide the greatest potential benefit for high-density, high-speed and low-voltage integrated circuit (IC) chip packaging. Capacitors can be embedded into the interconnect substrates to provide decoupling, bypass, termination, and frequency-determining functions **[2, 3]**. In order for embedded capacitors to be useful, the capacitor must be flexible as well as show high capacitive densities to make layout areas reasonable. Available commercial polymer composite technology is not adequate for flexible high capacitance density thin film embedded passives. Several polymer nanocomposite studies have focused on processing of thin films with high capacitance density within small substrates/wafers **[4-7]**. One of the important processing issues in thin film polymer nanocomposite based capacitors is to achieve flexibility and high capacitance density with large-area coatings.

In this paper, we report novel barium titanate ($BaTiO_3$)-polymer based nanocomposites that have the potential to surpass conventional composites to produce thin film capacitors over large surface areas, having high capacitance density and low loss. Specifically, the focus is on new flexible composite dielectric materials that can be integrated into boards, laminate chip carriers (LCCs), or roll-to-roll manufacturing processes. A variety of nanocrystalline $BaTiO_3$ powders were utilized with the objective of manufacturing low-cost, high-performance, flexible nanocomposites with subsequent laser micromachining of the nanocomposites to produce novel micromachined 3D capacitors. Micromachining technologies can produce variable thickness and discrete capacitors from a single sheet (layer) of capacitors and could be integrated in the same layer (**Figure 1**). Moreover, an improved micromachining technique was developed to control the surface morphology of sol-gel thin films. Experimental data shows micromachining is highly efficient for controlling film thickness. With this method, new structures can be designed without altering the dielectric properties of the nanocomposites. The tec;hnique can be used to generate multi-functional capacitors.

1. Experimental Procedure

A variety of $BaTiO_3$ nanoparticles and their dispersion into epoxy resin were investigated in order to achieve a thin uniform film. In a typical procedure, $BaTiO_3$ epoxy nanocomposites were prepared by mixing appropriate amounts of the $BaTiO_3$ nano powders and epoxy resin in organic solvents. A thin film of this nanocomposite was then deposited on a copper substrate and cured. Barium titanate ($BaTiO_3$)-epoxy polymer nanocomposites modified with nanomaterials were also prepared. Various nanomaterials including PZT (lead zirconate titanet), PLZT (lead lanthanum zirconate titanate), ZnO (zinc oxide), PMN (lead magnesium niobate), PMN-PT (lead magnesium niobate-lead titanate) and

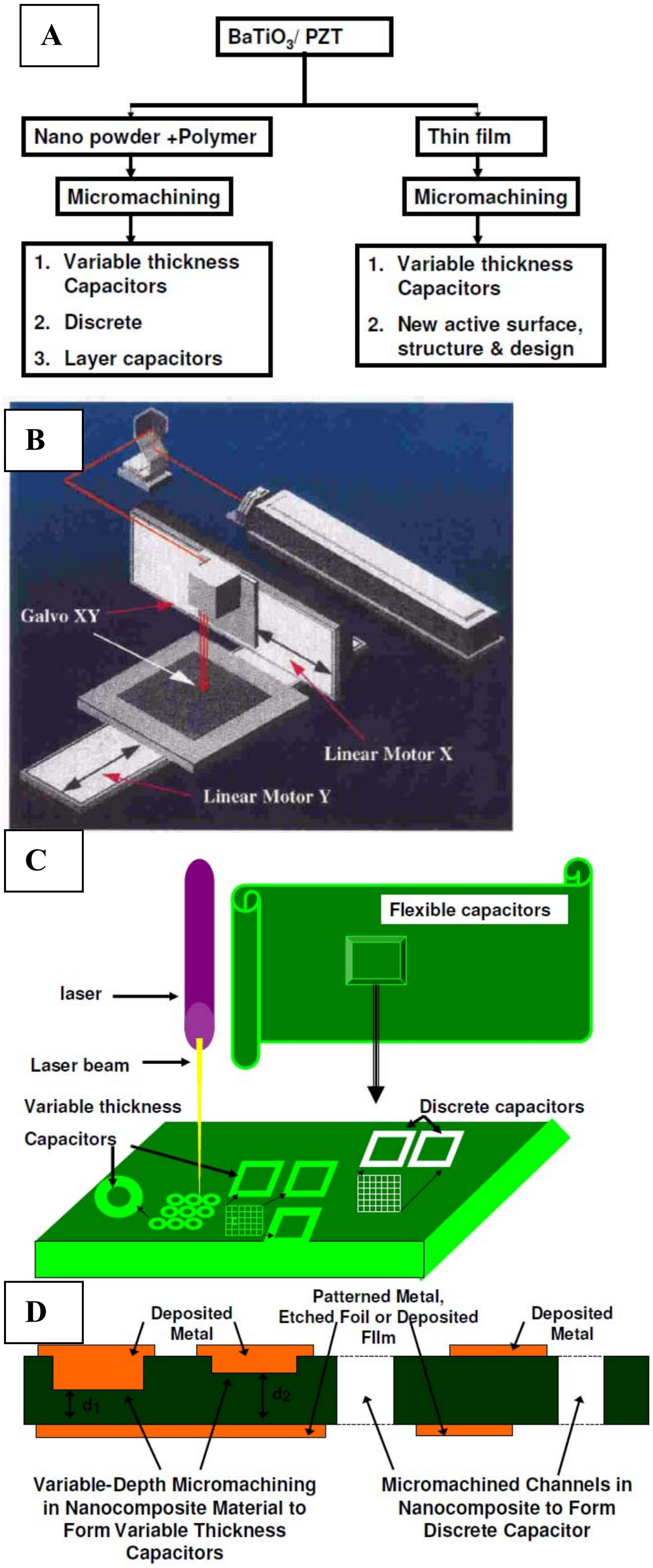

Figure 1: Schematic representations (A) process flow chart, and (B) laser processing (source: ESI), and (C)-(D) micromachining : top and cross sectional views showing arrays of discrete and variable-thickness capacitors.

several other single and multicomponent systems were used. Preparation of nanomaterials were discussed in previous papers [**8-11**]. $BaTiO_3$ fluoropolymer nanocomposites were also prepared by mixing appropriate amounts of the $BaTiO_3$ nano powders and fluoropolymer in organic solvents.

In the case of laminates, two thin films were prepared, dried, and then laminated together. $BaTiO_3$-sol-gel thin films were prepared from a 0.5 molar aqueous acetate solution of $Ba(CH_3COO)_2$ and $Ti(OC_2H_5)_4$. The film was deposited on Si or glass substrates by spin coating, and dried successively at 150° and 450°C to remove all the organics. The film was then annealed at ~600°C in air to generate a crystalline phase.

2. Laser Parameters and Micromachining Results

Laser drilling was performed on an ESI (Electro Scientific Industries, Inc., Portland, OR) 5210 Laser Microvia Drill System. A frequency-tripled Nd:YAG laser operating at a wavelength of 355 nm was used. The pulse width of the laser was on the order of 50 ns. The beam was positioned relative to the surface of the workpiece by coordinated motion of the stage on which the sample is mounted (y-axis), the optics (x-axis), and galvo mirrors (x and y axes), as shown in **Figure 1**. The position of the sample with respect to the focal plane of the imaged laser beam (along the z-axis) can also be adjusted. The spatial distribution of energy in the circular laser spot is homogenized by use of ESI-supplied optics. In this instance, beam diameter at the surface of the workpiece was varied by adjusting the relative position of the imaged beam with respect to the surface of the film. Other salient parameters are listed in the table below. Parameters are defined as follows.

Rep Rate is the number of laser pulses delivered to the workpiece per unit time.
Power is the average power of the laser.
Z-Offset is the relative position of the imaged beam with respect to surface of the substrate; a negative number indicates that the beam is imaged below the surface.
Velocity is the speed at which the beam is traced along the programmed beam path.
Repetitions is the number of times the system traces the programmed beam path.
Bite Size is the distance the system moves the beam relative to the workpiece between pulses, along the programmed beam path.

Direct laser ablation of nanocrystalline $BaTiO_3$ filled epoxy was performed using the parameters given in the table below. The $BaTiO_3$ filled epoxy nanocomposite and sol-gel thin film were micromachined using a variety of conditions to form various surface morphology and capacitors arrays .

Material Thickness (um)	2.5	8.5
Power (watts)	0.3	0.3
Z-Offset (mm)	-0.45	-0.45
Rep Rate (kHz)	12	12
Repetitions	4	13
Bite Size (um)	8.33	8.33
Velocity (mm/sec)	100	100

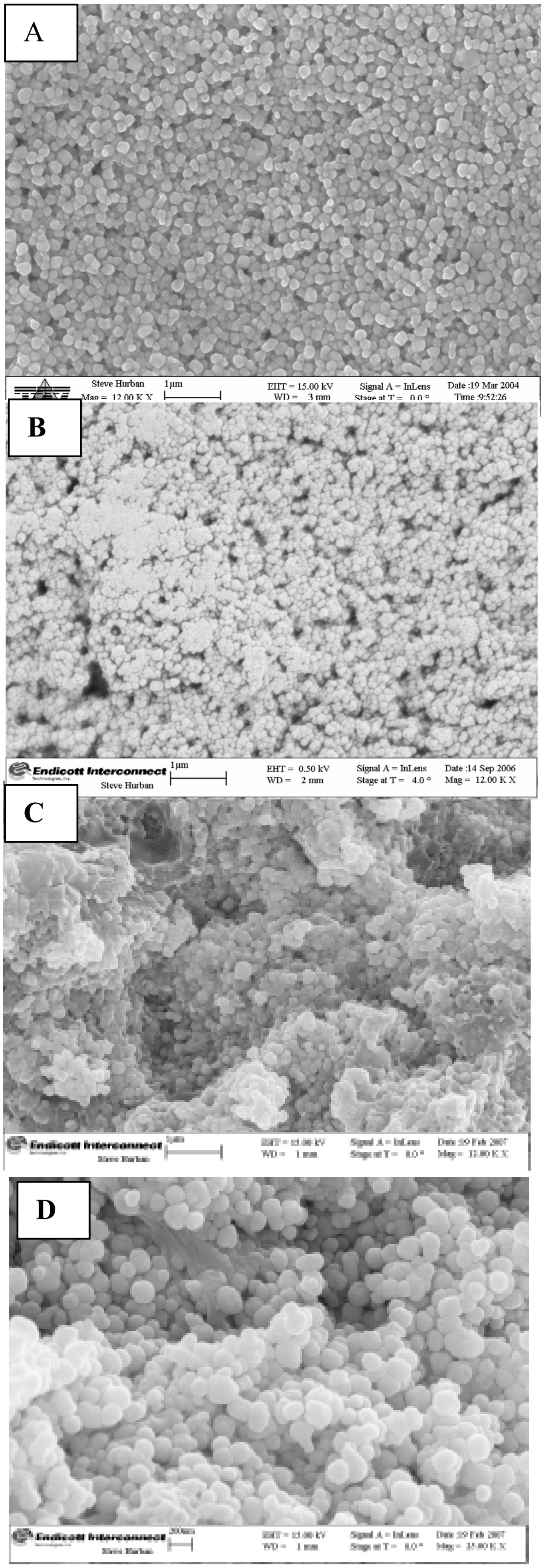

Figure2: Larger area SEM micrographs of (A) $BaTiO_3$-epoxy polymer nanocomposites, and (B) nanomaterials-modified barium titanate $BaTiO_3$-epoxy polymer nanocomposites, and (C)-(D) $BaTiO_3$-Fluoropolymer nanocomposites.

Electrical properties (capacitance, Dk, loss) of the nanocomposite thin films were measured at room temperature using an impedance/gain-phase analyzer (Model 4194A, HEWLETT-PACKARD). Surface morphology and particle distributions of nanocomposite films were characterized by a LEO 1550 scanning electron microscope (SEM). Micromachining depths of films were determined by optical microscope and SEM.

3. Results and Discussion

A real challenge in the development of large area thin film nanocomposites is the incompatibility that exists between the typically hydrophilic nanoparticles and hydrophobic polymer matrix. This leads to nanoparticle agglomeration. As a result, inferior coatings with poor performance are obtained. Surface treatments that result in excellent dispersability of the nanoparticles, and good quality, monolithic coatings have been identified. Surface treatment of ceramics depends on their processing history.

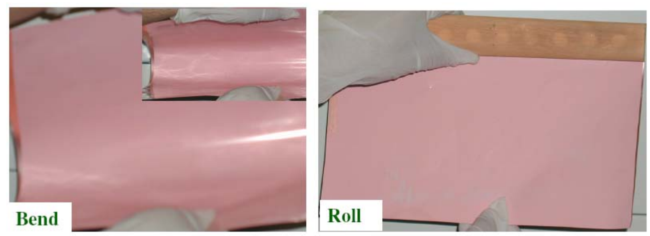

Figure 3: Flexible and rolled capacitors (Inset: bending at ~45degree).

Ramesh et al [7] reported silane treatment of hydrothermally prepared $BaTiO_3$ nanoparticles. The finer details of the particles and their surface morphologies have been investigated using SEM. **Figure 2** shows SEM micrographs of nanocomposite thin films. Nanoparticles formed a uniform dispersion in the epoxy matrix (**Figures 2A-2B**). The particles in the epoxy matrix are so intimately compacted that analysis of individual particles is difficult. However, closer observation of the micrographs clearly reveals a uniform distribution of closely packed, well connected particles. The uniform dispersion of nanoparticles into the epoxy matrix enables formation of a very thin film. The SEM micrographs shown in **Figures 2C and 2D** show the microstructure $BaTiO_3$ nanoparticles dispersed into a flexible fluoropolymer. **Figure 3** shows large area, thin flexible capacitors. Capacitors can be bent or rolled without damaging the structure. For conventional composites, rolling or bending will cause structural damage such as cracking. The remarkably increased flexibility of the nanocomposite is due to uniform mixing of nanoparticles in the polymer matrix and the resulting improved polymer-ceramic interface. Integration of this flexible capacitance layer into a flexible structure could be useful for developing high-performance multilayer flexible electronics, such as roll-up displays, e-papers, and keyboards.

Measurement of electrical properties of capacitors fabricated from nanocomposite thin films and having areas of ~2-100 mm^2 showed high capacitance density ranging from 10 $nF/inch^2$ to 100 $nF/inch^2$, depending on composition, particle size, and thickness of the coatings. Thin film capacitors fabricated from 40-60% v/v $BaTiO_3$ epoxy nanocomposites showed a stable capacitance density in the range of 40-80 nF/inch^2. Measurement of electrical properties of capacitors fabricated from ~70% v/v nanocomposite showed capacitance density of about 100 nF/inch^2. Capacitance density of $BaTiO_3$-epoxy polymer nanocomposites modified with nanomaterial was also investigated. The final film was assumed to have nanomaterials incorporated homogeneously into a $BaTiO_3$-epoxy matrix. Capacitance density of nanomaterials modified films were 500 nF/inch^2, about 5-10 times higher than obtained with $BaTiO_3$-epoxy nanocomposites.

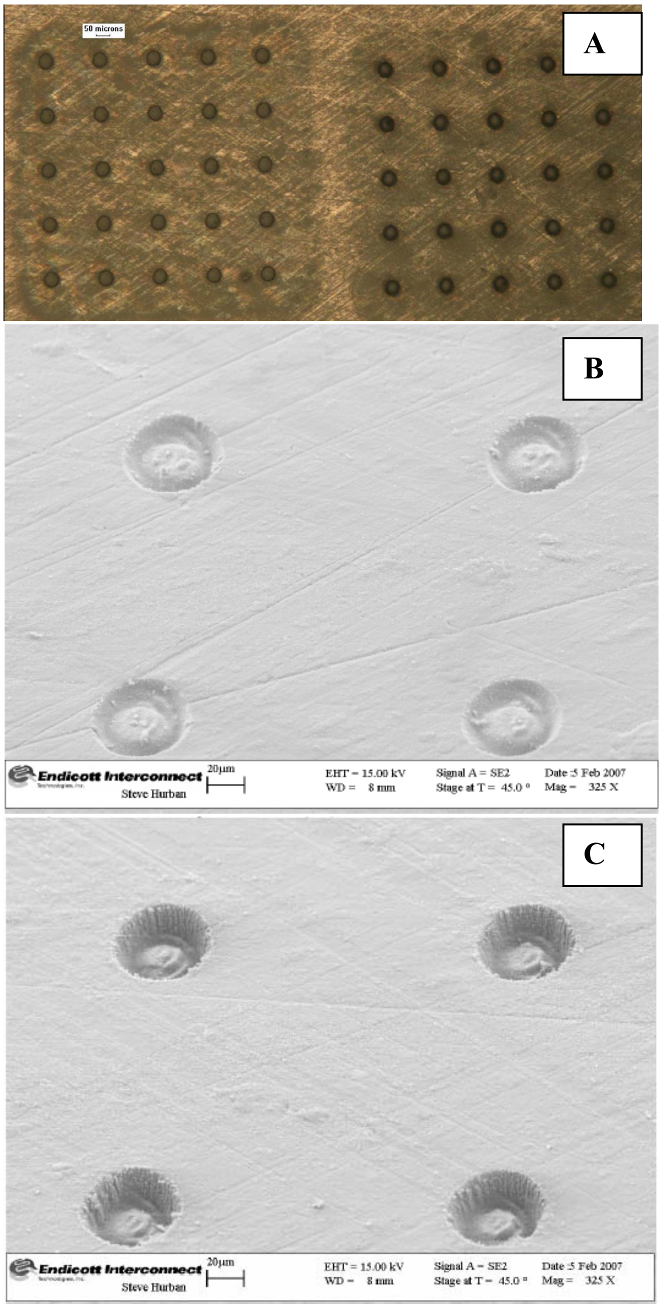

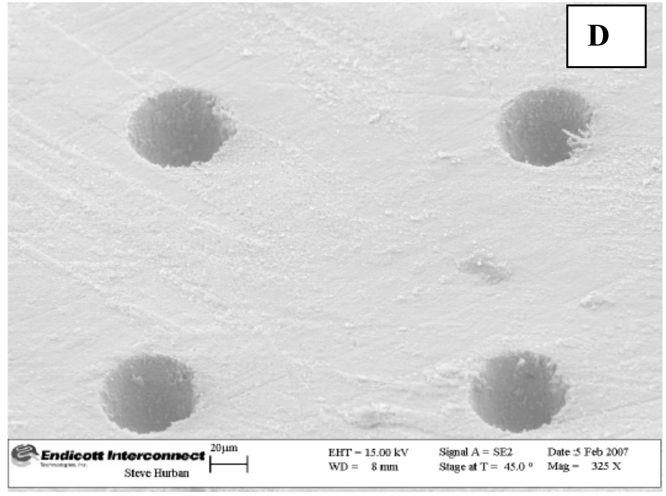

Figure 4: Micromachined nanocomposite based capacitor array (A) Optical photograph, (B) SEM micrograph of array machined with 20 pulses, (C) micrograph of array machined with 50 pulses, and (D) micrograph of array machined with 200 pulses.

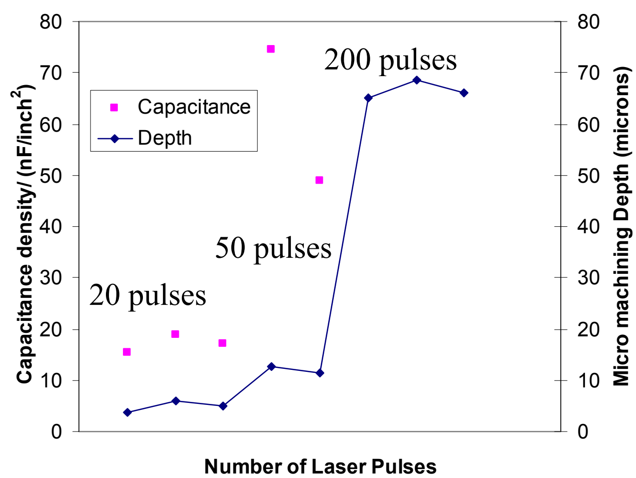

Figure 5: Variation of depth with the number of laser pulses for a $BaTiO_3$ nanocomposite (Dk =30). Theoretical calculation of capacitance change with number of laser pulses for nanocomposite thin film (Dk =30, thickness = 15 micron).

Figure 4A shows a top view of laser micromachined capacitor arrays. The basic structure consists of two layers: the micromachined capacitor and the glass substrate. Using this method, fully micromachined capacitors can be consistently generated. SEM micrographs are shown in Figures 4B to 4D for a series of arrays machined using varying numbers of laser pulses. The depth of microfabricated capacitors varies from 4 microns to 70 microns, depending on the number of laser pulses. The surface smoothness of the ablated areas that define the laser micromachined capacitors depends upon the uniformity of the spatial energy distribution of the laser beam . Although the smoothness of the ablated regions shown in Figure 4 are not optimum, adjustment of the optics used in the present study could produce a more homogeneous energy profile for the beam. Alternatively, excimer laser micromachining systems have been shown to produce very uniform ablation over reasonably large areas. Yet another potential alternative is to micromachine a b-staged dielectric material, and smooth the micromachined surface during a final composite lamination.

Figure 5 shows variation of the depth of the micromachined areas with the number of laser pulses. **Figure 5** also shows possible capacitance density (nF/inch^2) for a 15 micron capacitor film assuming a dielectric constant 30. The thickness of the capacitrors decreases with an increasing number of laser pulses. It is clear from **Figure 5** that as the depth of the micromachined area is increased (thickness of the remaining dielectric reduced), the corresponding capacitance increases In other words, micromachining can generate capacitor libraries with variable capacitance density. Increasing the number of pulses eventually results in complete removal of the dielectric. This would be useful for making discrete capacitors from a capacitance layer. **Figure 6** shows a representative example of discrete capacitors formed from a larger capacitance layer. Figure 6B represents a 3D optical micrograph where the capacitor dielectric was to the point where the bottom electrode was exposed.

For $BaTiO_3$/PZT based sol-gel thin film exposed to high energy density, material absorption favors ablation. On the other hand, when sol-gel thin films are exposed to the same laser at low energy density, material absorption favors annealing.

The surface topography of the $BaTiO_3$ thin film surfaces was examined by performing AFM, SEM, and optical imaging. **Figure 7** shows different surface morphology generated by variation of laser fluence. Sufficiently strong laser pulses induce local melting and rapid cooling, leading to formation of an amorphous particle. One can use laser irradiation to raise the temperature of the film above the crystallization temperature, but below the melting temperature, thus converting an amorphous region to a crystalline phase. **Figures 7A and 7B** represent typical examples of melting and solidification of amorphous particles. Ablation was observed at very high energy densities. With a gradual decrease in energy, but still at high enough fluence values, the central part of the area traced by the laser beam path completely melts, whereas the adjacent surrounding area appears to be partially melted.

Laser processing of the as-deposited $BaTiO_3$ film leads to a noticeable conversion from a smooth surface to wavy cavity structure as can be seen in the SEM and optical images (**Figures. 7C, D, E**). This is apparently due to local melting of the top surface induced by the transient laser heating. Similar melting behavior has been observed in pulsed laser deposition of ZnO films upon laser annealing at 193 nm **[12]**. The annealing substantially reduces the surface grain structure and generates a new porous channel-like network reminiscent of a labyrinth structure. Each channel has an average width of about 2-5 microns and depth of about 0.1-0.5 micron. It is interesting to note that all the laser-annealed/micromachined spots, irrespective of their location on the film (center or periphery), maintain almost the same kind of channel structure. Moreover, it can be created in selective locations. This kind of structure was shown to be critical for achieving laser like action upon optical pumping as it favors efficient coupling of the pump light into the film material [**13**]. Excess laser energy favors ablation. It can be seen that at high laser energy, the barium titanate film is ablated and the underlying silicon surface exposed (**Figure 7F**).

Laser micromachining is important for generating high resolution patterns. In contrast to many patterning techniques, this approach does not necessarily require toxic chemicals. **Figure 8** shows a simple micromachined pattern composed of letters, lines, and a square grid. The vertical lines were positioned on a 200 µm pitch (left side) and a 100 µm pitch (right side). The length and width of these sides of the squares in the grid is 200 µm. Line widths in all cases are 50 µm. The laser can be used to machine a small gaps for micro devices. For instance, one can machine small planar energy storage devices for remote sensors in security or defense applications. The AFM image shown in **Figure 9** represents a sharp michomachined $BaTiO_3$ edge at the glass surface. This kind of sharp edge will be useful for microfabricating membranes for MEMS applications [**14**]

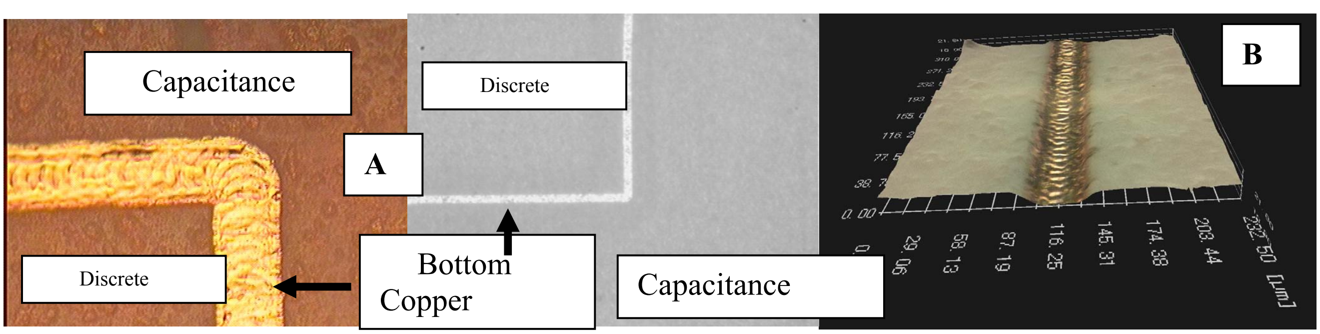

Figure 6: Laser micromachining produces discrete capacitor from a capacitance layer (A) Optical photograph (B) Optical 3D photograph of another sample.

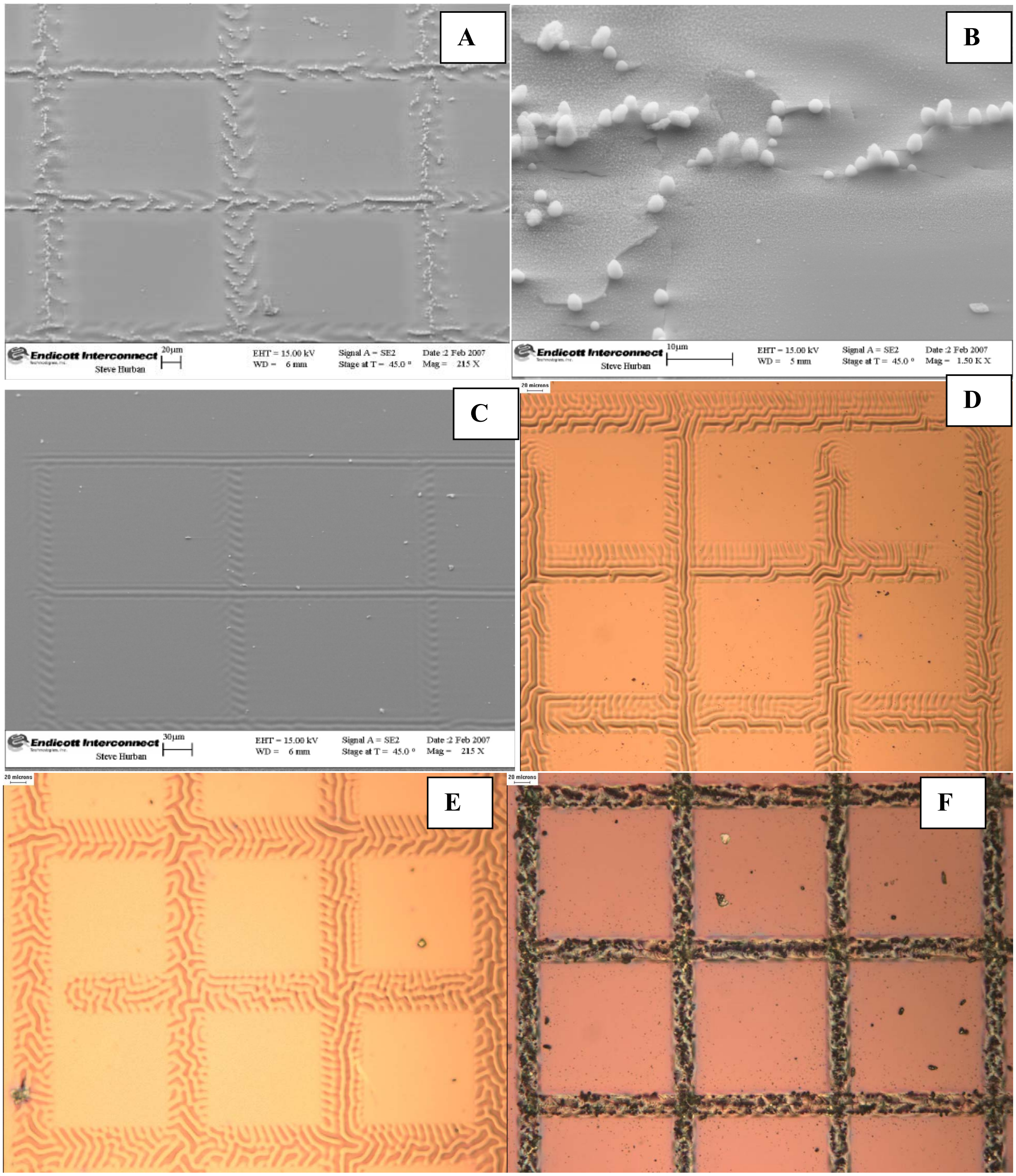

Figure 7: SEM micrographs and optical photographs of laser micromachined sol-gel thin films; (A) and (B) Low and high magnification SEM micrographs of thin films with surface particles, (C) to (E) SEM micrograph and optical phtotographs of thin films with a wavy, channel-like structure, and (F) Optical photograph of a micromachined (ablated) thin film surface for which the sol-gel thin film has been completely removed in the channels..

4. Conclusions

A thin film technology based on $BaTiO_3$-epoxy polymer nanocomposites was developed to manufacture high-performance, large-area, flexible/rollable, thin film capacitors. It is possible to produce very thin films, on the order of 2 microns, using the nanocomposites. The remarkable flexibility and thickness of the nanocomposite is due to uniform mixing of nanoparticles in the polymer matrix which results in improved polymer-ceramic interfaces. A frequency-tripled Nd:YAG laser operating at a wavelength of 355 nm was used for the micromachining study. We have shown a variety of micromachined surfaces suitable for multifunctional capacitor applications. Lasers can provide various complex micromachined patterns. This technique can be used to prepare capacitors of various thicknesses from the same capacitance layer, and ultimately can produce variable capacitance density, or a library of capacitors. The process is also capable of making discrete capacitors from a single layer of capacitance material. As the demand grows for complex multifunctional embedded components for advanced organic packaging, laser micromachining will continue to provide unique opportunities.

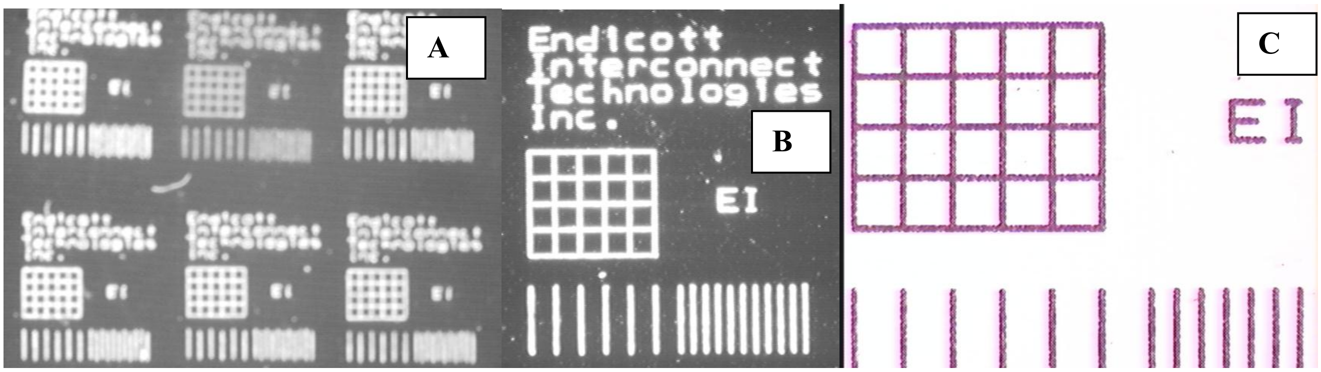

Figure 8: Optical micrograph of micro fabricated complex structures (A) low magnification and (B) high magnification, and (C) Bright field high magnification.

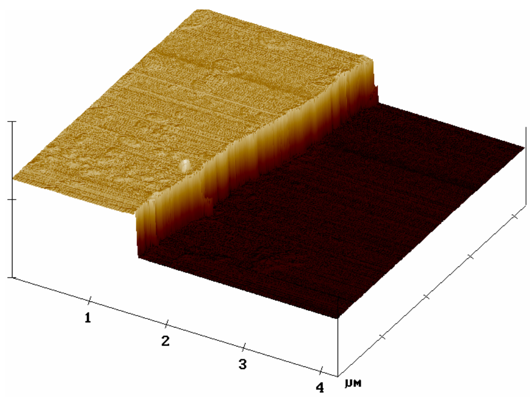

Figure 9 : AFM image micromachined $BaTiO_3$ thin film.

References:

1. J. M. Bustillo, R. T. Howe, and R. S. Muller, "Surface micromachining for microelectromechanical systems," *Proc. IEEE*, vol. 86, pp. 1552–1574, 1998.
2. "Passive Integration: Easier Said Than Done", Prismark Partners LLC, August 1997
3. Post J. E., "Microwave performance of MCM-D embedded capacitors with interconnects" *Microwave and Optical Technology Letters* Vol. 46, No5, (2005), pp. 487-492.
4. Rao Y., Ogitani S., Kohl P., Wong C. P., "Novel polymer-ceramic nanocomposite based on high dielectric constant epoxy formula for embedded capacitor application" *Journal of Applied Polymer Science* Vol. 83, No. 5, (2002), pp.1084-1090.
5. Rao Y., Wong C. P., " Material characterization of a high-dielectric-constant polymer-ceramic composite for embedded capacitor for RF applications" *Journal of Applied Polymer Science* Vol. 92, No. 4, (2004), pp. 2228-2231.
6. Windlass H., Raj P. M., Balaraman D., Bhattacharya S. K., and Tummala R. R., " Colloidal processing of polymer-ceramic nanocomposites for integral capacitors" *IMAPS International Symposium on Advanced Packaging Materials*, Braselton, 2001, pp. 393-398
7. Ramesh S., Shutzberg B. A., Haung C., Gao J., Giannelis E. P., "Dielectric nanocomposites for integral thin film capacitors: Materials design, fabrication, and integration issues" *IEEE Transactions on Advanced Packaging* Vol. 26, No. 1, (2003), pp. 17-24.
8. R.N. Das, A. Pathak and P. Pramanik, "Low-Temperature Preparation of nanocrystalline Lead Zirconate Titanate and Lead Lanthanum Zirconate Titanate Powders Using Triethanolamine" Journal of American Ceramic Society 81[12] 3357-60(1998).
9. R. N. Das and P. Pramanik, "Single step Chemical Synthesis of Lead Based Relaxor Ferroelectric Niobate Fine Powders" Nanostructured Materials 11[3] 325-330 (1999).
10. R.N. Das and P. Pramanik,"In situ synthesis of nanosized PZT powders in the precursor materialand the influence of particle size over the dielectric property" Nanostructured Materials10 [08] 1371-1377(1999).
11. R. N. Das and P. Pramanik, "Chemical Synthesis of Nanocrystalline $BaTiO_3$ and $Ba_{1-x}Sr_xTi_{1-y}Zr_yO_3$ [(i) x=0.03, y=0 (ii) x=0, y=0.03] Ceramics " Nanotechnology, 15, 279-282, 2004I.
12. Ozerov, M. Arab, V. I. Safarov, W. Marine, S. Giorgio, M. Sentis, L. Nanai, "Enhancement of exciton emission from ZnO nanocrystalline films by pulsed laser annealing" Appl. Surf. Sci., 226 (2004) 242.
13. A. Stassinopoulos, R. N. Das, E. P. Giannelis, S. H. Anastasiadis, D. Anglos "Random lasing from surface modified ZnO films of ZnO nanoparticles" Applied Surface Science,2005,247,18-24
14. Hai Ni, Hoo-Jeong Lee, Ainissa G. Ramirez, "A robust two-step etching process for large-scale microfabricated SiO2 and Si3N4 MEMS membranes" Sensors and Actuators A 119 (2005) 553–558